ENHANCED CONTROL STRATEGY OF THREE-PHASE VOLTAGE SOURCE INTERACTIVE INVERTER USING MODEL PREDICTIVE CONTROL STRATEGY

Misbawu Adam[1], Adjei-Saforo Kwafo Edmund[1,2], Samuel Addo Darko[1], Solomon Nchor Akansake[3]

[1]*Faculty of Engineering and Technology, Kumasi Technical University, Kumasi*

[2]*Faculty of Computer and Electrical Engineering, COE, KNUST, Kumasi.*

[3]*Faculty of Physical Sciences Computational Sciences, COS , KNUST, Kumasi.*

Abstract

A lot of techniques based on active power filter have been proposed in many transmission and distribution networks for harmonic mitigation. However, this does not come easy as it may involve a chain of cascaded structures coupled with large computational data, which consequently affects the response of the control system. In this paper, model predictive control (MPC) strategy based on active power filter (APF) is proposed to accomplish the real-time and accurate harmonic current compensation in the power systems. In MPC strategy, the future behaviour of the controlled variables is predicted using the model of the system. The cascaded structure usually applied in linear control system is avoided, giving rise to a fast response. Verification of the effectiveness and validity of the proposed method are demonstrated by the simulation results using MATLAB/Simulink tools. The results show a significant reduction in the Total Harmonic Distortion (THD) when sampling time is varied.

Keywords: *Total harmonic distortion, model predictive control, Active power filter, Nonlinear loads.*

1.0 INTRODUCTION

Recently, power electronic devices such as static power converters, electric arc furnace and others which draw nonlinear currents are extensively used for commercial and industrial purposes. These devices, when connected to the grid generate multiple integral frequency waveforms which have the tendency to deform the original voltage and current waveforms giving rise to power quality issues. [1-2]. Current or voltage sources with high harmonic contamination can lead to power dissipation as a result of heating effect, mis-operation and dis-operation of power system equipment. Currently, special sophisticated device which can optimally counterbalance for reactive power, harmonic current contamination as well as to eliminate the asymmetrical loads is the active power filter (APF). Control strategy for voltage source inverter (VSI) cannot be overemphasized in the compensation performance of an APF [3]. With reference to voltage source inverter, varietal control strategies have been researched on [4-7]. However, these techniques involve complex

calculation and their implementations are very sophisticated and long-delayed. Again, the hardware implementation requires high processing capabilities.

In recent times, model predictive controls (MPC) have found application in semiconductor embedded devices. In classical control strategies, the MPC owing to its simple concept and swift dynamic response, has become attractive in its field of endeavour. In accordance with its control algorithm, varietal techniques have been produced under its name [8-10]. The finite control set MPC (FCS-MPC) is a very flexible control scheme and simple that permits the effortless inclusion of constraints and nonlinearities in the design protocol of the controller. In addition, modulator is not required in the designed scheme. This technique has been successfully applied in broad spectrum of semiconductor embedded converters [11-14].

In this paper, an MPC for the control of two-level three-phase voltage source inverter based on APF is presented. The first aspect of the MPC technique is the use of the future prediction to create control input based on different possibilities. The second aspect is the use of the cost function to carry out a precise calculation to minimize error, which is called the optimization stage. Authors in [15] presented predictive current control strategy for a grid-connected four-leg inverter. A similar approach is adapted in this paper to control the two-level three-phase inverter based APF. MATLAB/Simulink is used to determine the veracity of the proposed strategy in APFs.

2.0 TWO-LEVEL THREE-PHASE INVERTER TOPOLOGY

A circuit diagram of the VSI with DC-link inclusive used in this work is shown in Figure 1. Let the gate signals 1 or 0 represents the position of the switch for a phase, with S_a, S_b and S_c and their complement used to describe the switching states. The only possible control actions used are the ones generated by the model switching states since no modulator is used in MPC. The phase voltages are given by

$$V_{xN} = \begin{cases} V_{dc}, & if\ S_x = 1 \\ 0, & if\ S_x = 0, \end{cases} \quad (x = a, b, c) \tag{1}$$

There exist ($2^3 = 8$) different voltage vectors since there are eight switching states. The real voltage at the inverter terminal is determined using

$$V = {}^{2}/_{3}\,(V_{aN+}\alpha V_{bN} + \alpha^2 V_{cN}) \tag{2}$$

as summarized in Table 1, where $\alpha = 120^o$ phase displacement between the phases. In this way, the switching states are used to generate the voltage vectors

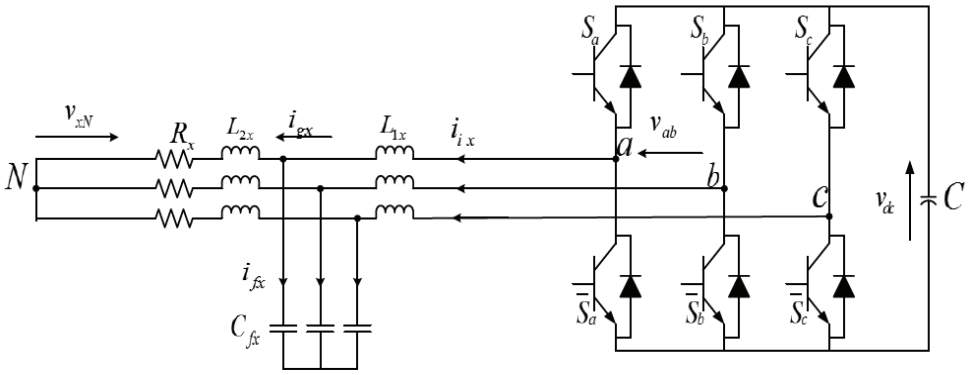

Figure 1: The 2-level 3-phase voltage source inverter

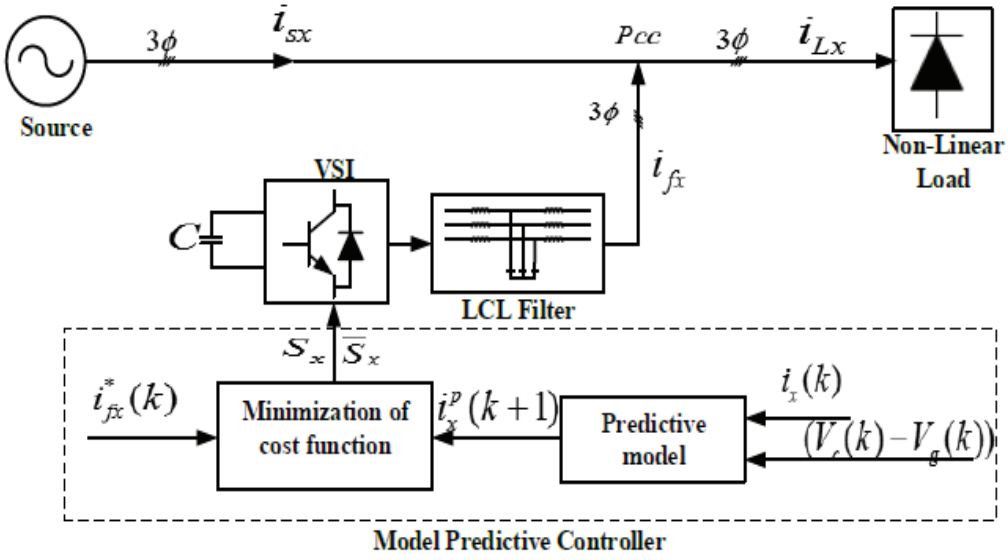

Figure 2: Block diagram of the proposed MPC scheme

2.1 Load Model

It is important to take into account the definition of variables from the inverter circuit shown in Figure1, in order to determine the load model of the system. According to [16], since the impedance of the capacitor (C_f) is very large relative to, L_1 and L_2 the current through it can be ignored. Hence total reactive impedance

$$L = L_1 + L_2 \qquad (3)$$

can be obtained from Figure 1, and the dynamic model of the inverter can also be expressed by

$$V_c = V_g + Ri + L\frac{di}{dt}, \qquad (4)$$

a differential equation as in [17]. Where V_g and V_c are the grid side and generated inverter voltages respectively and, R and L vector-summation gives the load impedance.

Table 1: Switching states and voltage vectors

No	S_a	S_b	S_c	Voltage Vector V
1	0	0	0	$V_0 = 0$
2	0	0	1	$V_1 = -\left(\frac{1}{3} + j\frac{\sqrt{3}}{3}\right)V_{dc}$
3	0	1	0	$V_2 = -\left(\frac{1}{3} - j\frac{\sqrt{3}}{3}\right)V_{dc}$
4	0	1	1	$V_3 = -\left(\frac{2}{3}\right)V_{dc}$
5	1	0	0	$V_4 = \left(\frac{2}{3}\right)V_{dc}$
6	1	0	1	$V_5 = \left(\frac{1}{3} - j\frac{\sqrt{3}}{3}\right)V_{dc}$
7	1	1	0	$V_6 = \left(\frac{1}{3} + j\frac{\sqrt{3}}{3}\right)V_{dc}$
8	1	1	1	$V_7 = 0$

2.2 Model Predictive Current Control Strategy

A block diagram of the proposed MPC structure is depicted in Figure 2. Basically, the technique requires hardware microprocessor-based. As a result, discrete mathematics is used for its analysis in order to consider restrictions such as sampling time, approximations and delay [14]. Therefore, to predict the future trajectory, it is necessary to set up a model that captures the loads and constraints of the system. Since the dynamic model of the load of equation (5) is first order in nature, adapting Forward Euler method with concise sampling interval

$$\frac{di}{dt} \approx \frac{i(k+1)-i(k)}{T_s} \tag{5}$$

is usually sufficiently accurate and can be used to replace the load current $\frac{di}{dt}$ in (4). Then we obtain

$$i_x(k+1) = i_x(k)\left(\frac{L-RT_s}{L}\right) + \frac{T_s}{L}\left(V(k) - V_g(k)\right) \tag{6}$$

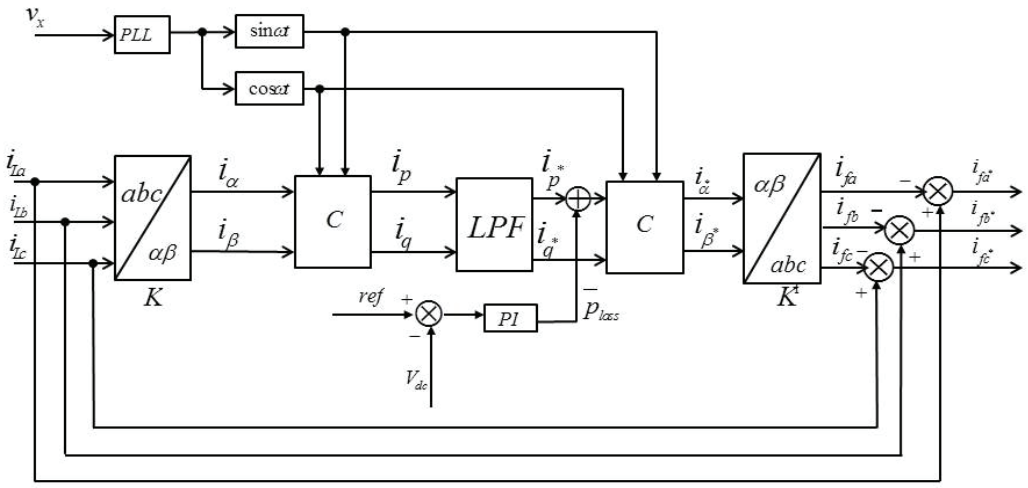

Figure 3: Reference current detection block diagram

An expression that predicts the future load current at (k + 1), for each of the voltage rectangular produced by the inverter. The estimated voltage

$$\hat{V}_g(k) = V(k) + i_x(k)\left(\frac{L-RT_s}{L}\right) - i_x(k+1)\frac{L}{T_s} \tag{7}$$

of $V_g(k)$ can be determined from (6).

2.3 Reference Current Detection Method

The i_p - i_q method based on instantaneous power theory is used in this work to detect the reference harmonic current components that is compared with the predicted current to determine the cost function which will be presented in the next section. This method was chosen because it effectively separates the fundamental current from the distorted current. Figure 3 shows the reference current detection diagram. The three-phase load current i_{lx} is transformed into α *and* β coordinates using the Clarke Transformation method. The i_p - i_q currents are obtained using the phase locked loop (PLL) module which generates sine and cosine signals with source voltage as its input. The reference current is detected through the following processes.

$$\begin{bmatrix} i_\alpha \\ i_\beta \end{bmatrix} = K \begin{bmatrix} i_a \\ i_b \\ i_c \end{bmatrix} \tag{8}$$

$$K = \sqrt{\frac{2}{3}} \begin{bmatrix} 1 & -0.5 & -0.5 \\ 0 & \frac{\sqrt{3}}{2} & -\frac{\sqrt{3}}{2} \end{bmatrix} \tag{9}$$

$$\begin{bmatrix} i_p \\ i_q \end{bmatrix} = C \begin{bmatrix} i_\alpha \\ i_\beta \end{bmatrix} \quad (10)$$

$$C = \begin{bmatrix} \sin \omega t & -\cos \omega t \\ -\cos \omega t & -\sin \omega t \end{bmatrix} \quad (11)$$

The split-second reactive and active DC-components of the current $i_p^* \; and \; i_q^*$ is determines as using a low pass filter.

$$\begin{bmatrix} i_\alpha^* \\ i_\beta^* \end{bmatrix} = C \begin{bmatrix} i_p^* \\ i_q^* \end{bmatrix} \quad (12)$$

Again, the current components of the fundamental are characterized as,

$$\begin{bmatrix} i_{fa} \\ i_{fb} \\ i_{fc} \end{bmatrix} = K' \begin{bmatrix} i_\alpha^* \\ i_\beta^* \end{bmatrix} \quad (13)$$

where $K' = \sqrt{\frac{2}{3}} \begin{bmatrix} 1 & 0 \\ -0.5 & \frac{\sqrt{3}}{2} \\ -0.5 & -\frac{\sqrt{3}}{2} \end{bmatrix}$ (14)

The reference current is obtained by

$$i_{fx^*} = i_{lx} - i_{fx} \quad (15)$$

subtracting the fundamental current from the distorted load current.

2.4 Optimization Function

This algorithm is used to compute all the seven possible conditions that the state variable can obtain during (k+1) instance. The switching position in the sampling instant (k) which reduces the error of the output current in sampling period is selected by the control technique. The achievement of the seven possible future predictions for i(k+1) sampling period is examined by the cost function.

$$g = \left| i_x^*(k+1) - i_x^p(k+1) \right| \quad (16)$$

to select the optimal switching state to be applied to the inverter. The cost function consists of $i_x^*(k+1)$, the reference current generated in the immediate above section and $i_x^p(k+1)$ the predicted current. The current error is given by the distinction between the reference

current and the current predicted in the phase leg. The choice of the input is established by current at *(k + 1)* . The equation (6) which defines a discrete model with all the admissible input is used to predict the current at *(k + 1)*. The switching state optimization, that is, the control input optimization at the instant *(k)* is obtained by minimizing the cost function *(g)*. Hence, optimization depends on the current $i(k)$ and the reference current $i^*(k+1)$. According to [14], the previous and present values of the reference current by means of a second-order extrapolation is derived from the Lagrange extrapolation function. This notwithstanding, for infinitesimal value of sampling period (T_s), it can be approximated to $i^*(k)$. The control algorithm is shown in the flowchart of Figure 5.

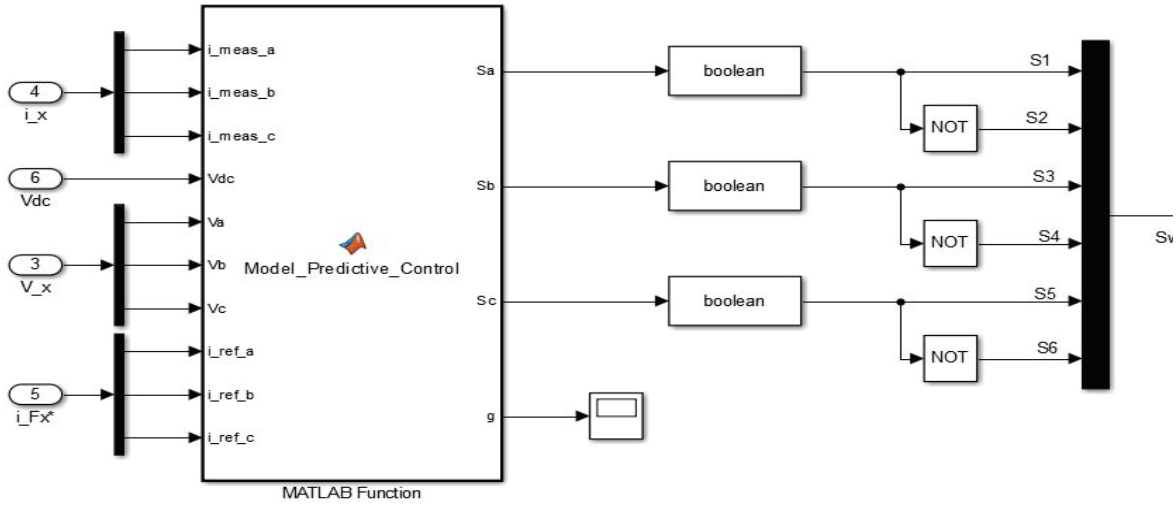

Figure 4: MATLAB/Simulink subsystem of MPC

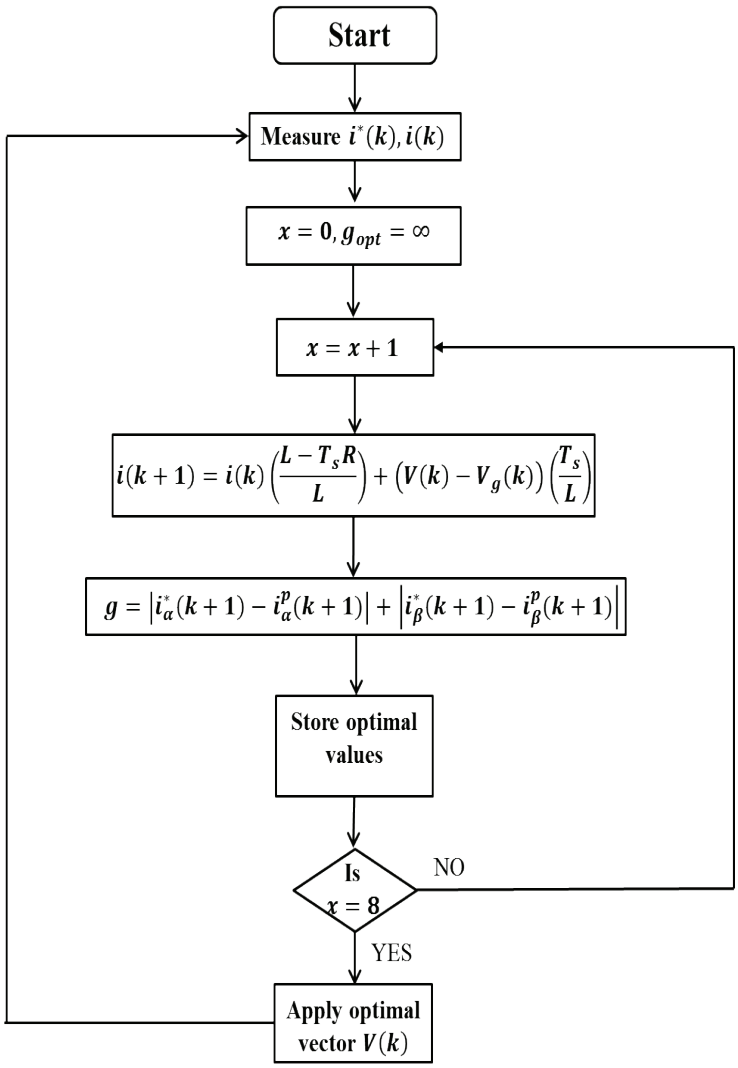

Figure 5: Control algorithm flow chart

3.0 SIMULATION AND PERFORMANCE EVALUATION

The performance is investigated according to the above analysis in MATLAB/Simulink, using the two-level three-phase inverter with LCL shown in Figure 1 and the subsystem of the MPC in MATLAB/Simulink is shown in Figure 4. The time delay is neglected because of controller computation. The parameters of the system are as follows:

the phase voltage $V_g = 220\ V$ is and the rated fundamental frequency $f_g = 50\ Hz$,

the load resistance $R = 10\Omega$, the total inductance $L = 2mH$,

the dc-link voltage $V_{dc} = 800V$, and

The sampling time is set to $T_s = 5\mu s$.

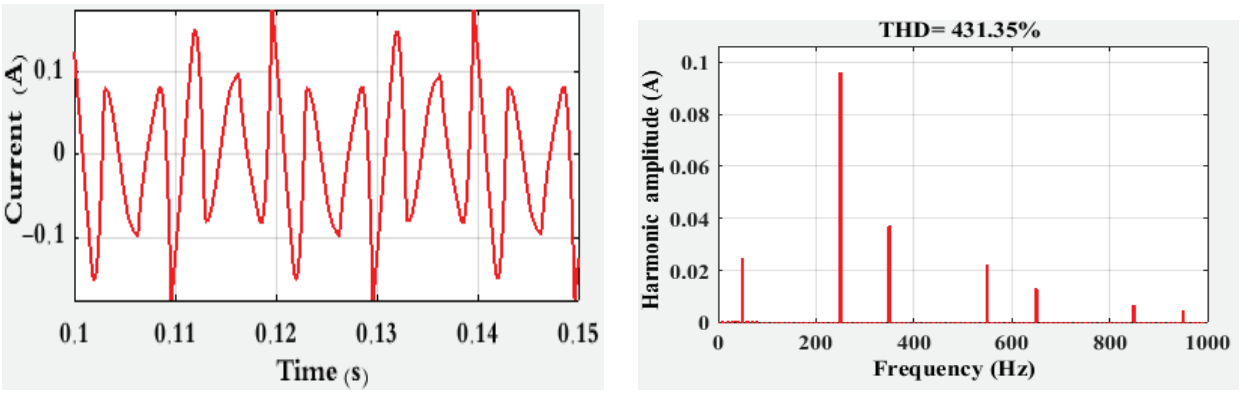

(a) Reference current waveform, *(b) Reference current spectrum*

Figure 6: Detected reference current for a single phase with THD=431.35%

The single-phase reference current waveform which is effectively separated from the fundamental current of the distorted load current is shown in Figure 6 (a). The resulting total harmonic distortion (THD) of the reference current is very high at THD=431.35% as shown in Figure 6 (b). The 5^{th}, 7^{th}, 11^{th}, and 13^{th} harmonic orders have high amplitude compared to the higher frequency harmonic orders.

Figure 7(a) shows the resultant waveforms of the source current before compensation, It must be noted that the load and source currents before compensation are the same. Figure7(b) shows the spectrum analysis of the source current. From the results, it can be seen that the source current has a THD of 23.49%. The highly distorted source current consists of a high 5^{th} harmonic order of 21.2%, the 7^{th}, 11^{th}, and 13^{th} harmonic orders have 8.06%, 4.9%, and 2.86% respectively of the fundamental current component which makes the waveform non-sinusoidal.

Figures 8 and 9 show the performance of the model predictive controller at sampling time respectively. Simulation waveforms of the source current after compensation have shown a drastic reduction in the harmonic current. As a result, it can be observed that the source current THD has reduced to 1.93% and 1.89% respectively with the 5^{th}, 7^{th}, 11^{th}, and 13^{th} harmonic orders at a very small percentage of the fundamental current component. The best control response is to obtain minimal THD. In particular when the THDs are less than the standard THD recommended by Std. IEEE 519, the value considered in the control design is the value that presents minimal THD. The controller, in both case, provides the best compensation possible, showing its effectiveness.

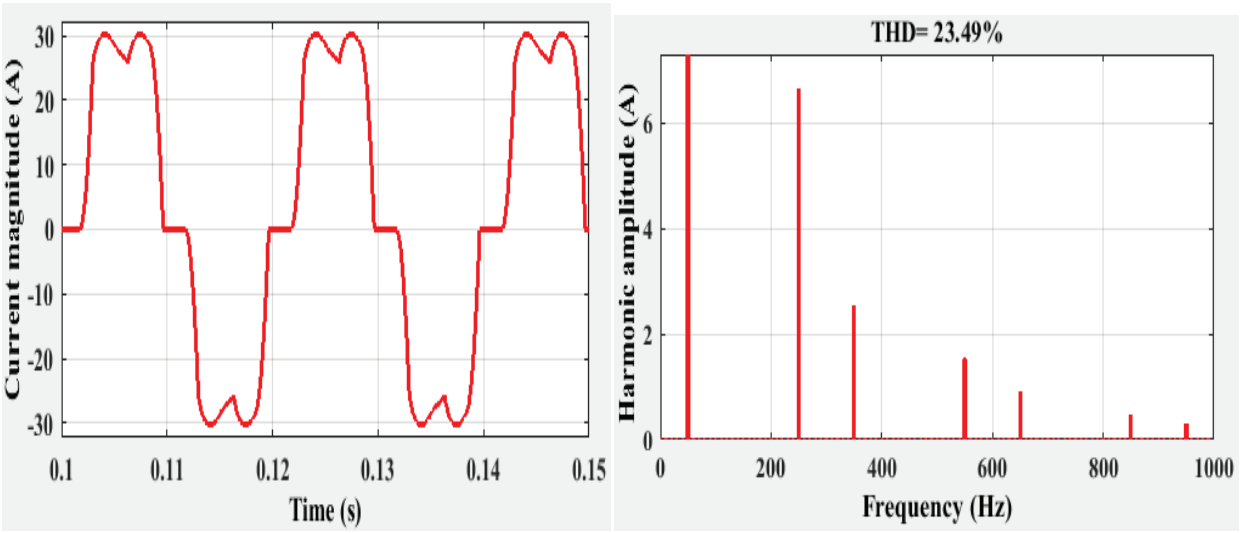

(a) Source current waveform *(b) Source current spectrum*

Figure 7: Source current for a single phase before compensation with THD=23.49%

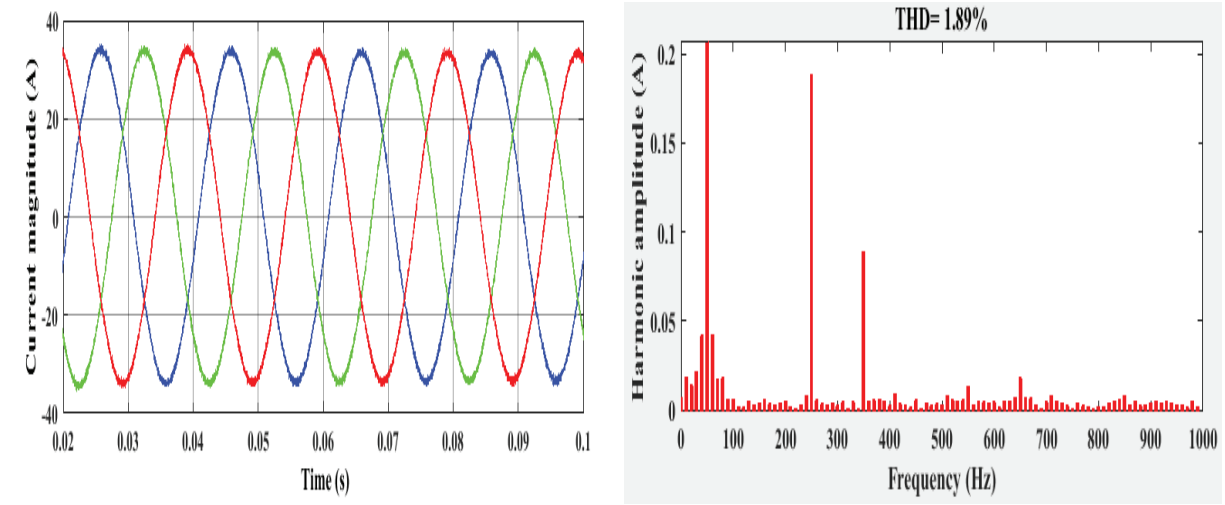

(a) Compensated current waveform *(b) Compensated current spectrum*

Figure 8: Three-phase Source current after compensation at $T_s = 2.5\mu s$ *with THD=1.89%*

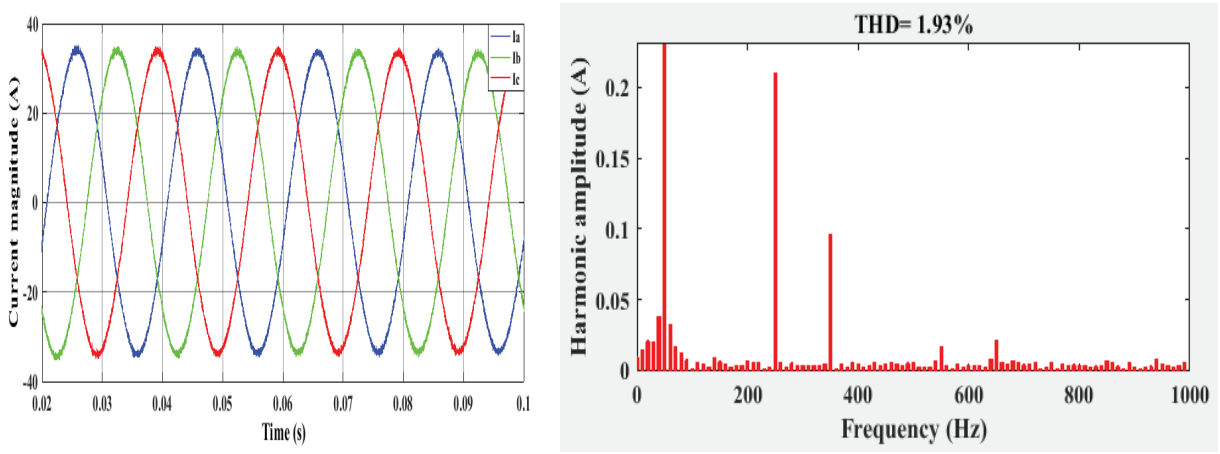

(a) Compensated current waveform *(b) Compensated current spectrum*

Figure 9: Three-phase Source current after compensation at $T_s = 2.5\mu s$ ***with THD=1.93%***

4.0 CONCLUSION

The idea of model predictive control applied to VSI based on APF has been introduced in the paper. This idea is used to compensate for the current harmonics generated by the extensive use of power electronic devices. This paper gave the description of the basic principle of MPC and proposed a novel design for control technique of an APF based on two-level three-phase inverter. MATLAB/Simulink platform has been used to design the APF and implement the proposed strategy. The simulation results demonstrated effectiveness of the presented strategy for APF. The method can enhance significantly electric power quality. By and large, the presented strategy does not only suppress harmonic but also it simplifies the calculation and can be auxiliarly applied as the modern control strategy of shunt active power filter.

REFERENCES

R. Li, J. Huang, and Z. Xu, "Active Harmonic Compensation Control for Nonlinear Loads Based on Disturbance Observer and Repetitive Control," in IEEE Transactions on Power Electronics, vol. 34, no. 4, pp. 3673-3684, Apr. 2019.

Y. Yu, M. Liu, and D. M. Vilathgamuwa, "A Hybrid Control Method for Harmonic Mitigation in Nonlinear Loads," in IEEE Transactions on Power Electronics, vol. 35, no. 1, pp. 876-886, Jan. 2020.

A. M. Abd-Elhady, M. M. Othman, and E. F. El-Saadany, "Modeling and Control of Nonlinear Loads in Distribution Networks for Harmonics Mitigation," in IEEE Transactions on Power Delivery, vol. 36, no. 3, pp. 1612-1623, Jun. 2021.

J. Tang, J. Li, and Z. Wang, "A Modified Control Method for Harmonic Compensation in Nonlinear Loads Based on Single-Phase Active Power Filter," in IEEE Transactions on Industrial Electronics, vol. 67, no. 1, pp. 211-221, Jan. 2020.

B. M. Gago, D. L. Maksimovic, and S. Cuk, "Analyzing Nonlinear Loads and Their Harmonic Contribution," \textit{IEEE Transactions on Power Delivery}, vol. 34,

no. 6, pp. 2456-2465, Nov. 2019.

M. R. Sharif, M. N. Marsono, and M. K. Khan, "Harmonic Modeling and Analysis of Nonlinear Loads," \textit{IEEE Transactions on Power Systems}, vol. 35, no. 2, pp. 1103-1114, Mar. 2020.

M. Lehtonen, A. Pääkkönen, and L. Kumpulainen, "Mitigation of Harmonics in Nonlinear Loads Using Model Predictive Control," in IEEE Transactions on Power Electronics, vol. 34, no. 3, pp. 2266-2277, Mar. 2019.

Rodriguez, J.; Cortes, P.: 'Predictive control of power converters and electric drives', Wiley-IEEE, Hoboken, NJ, USA, 2012, 1st edn.

Jiefeng, H., Ka, W.E.C.: 'Predictive control of power electronic converters in renewable energy systems', Energies, 2017, 10, pp. 1-14

Tien, H.N., Kyeong-Hwa, K.: 'Finite control set- model predictive control with modulation to mitigate harmonic component in t output current for a grid-connected inverter under distorted grid conditions', Energies, 2017, 10, pp. 1-25.

Jose, R., Marian, P. K., Jose, R. E., et al.: 'State of the art of finite control set model predictive control in power electronics', IEEE Transaction on Industry Informat., 2013, 9, pp. 1003–1016.

Ricardo, P. A., Pablo, L., Daniel, E.Q.: 'Finite-Control-Set model predictive control with improved steady-state performance', IEEE Transaction on Industry Informat., 2013, 9, pp. 658–667.

Luca, T., Pericle, Z., Alan, W., et al.: 'Modulated model predictive control for a three-phase active rectifier', IEEE Transaction on Industrial Application, 2015, 51, pp. 1610–1620.

Jose, R., Jorge, P., Cesar, A.S. A., et al.: 'Predictive current control of a voltage source inverter', IEEE Transaction on Industrial Electronics, 2007, 54, pp. 495 –503.

Jose, R., Wu, B., Rivera, M., et al.: 'Predictive current control of three-phase two-level four-leg inverter', Proc. 14th international power electronics and motion control conference, EPE-PEMC, 2010, pp.106-110.

Sung-Yeul, P., Jih-Sheng, L., Woo-Cheol, L.: 'An Easy, Simple, and Flexible Control Scheme for a Three-Phase Grid-Tie Inverter System', Proceedings of IEEE Energy Conversion Congress and Exposition, Atlanta, GA, USA, September 2010, pp.599-603.

Thai-Thanh, N., Hyeong-Jun, Y., Hak-Man, K.: 'Application of model predictive control to BESS for microgrid control'. Energies, 2015, 8, pp. 8798-8813.